Phase behavior of polymer blends with reversible crosslinks—A self-consistent field theory study

Thomas Gruhn[a)] and Heike Emmerich[b)]
Material and Process Simulation (MPS), University of Bayreuth, D-95447 Bayreuth, Germany

(Received 8 May 2013; accepted 10 October 2013)

An extended version of self-consistent field (SCF) theory that was recently introduced by the authors [Li et al., *J. Chem. Phys.* **137**, 024906, (2012)] is used to study the phase behavior of a polymer blend with reversible crosslinks. The system consists of symmetric *AB* diblock copolymers and homopolymers of type *A* and *B*. We consider reversible crosslinks that can form between the diblock copolymers with a crosslink strength z and crosslink weights ω_A and ω_B for monomers of type *A* and *B*, respectively. Crosslinks between homopolymers are disabled. We present a phase diagram as a function of the *A* fraction of homopolymers $\phi_\alpha^{\mathrm{rel}}$, the crosslink strength z, and the crosslink asymmetry $\Delta\omega = \omega_A - \omega_B$. A hexagonal phase is found for suitably large $\phi_\alpha^{\mathrm{rel}}$, and suitably small z and $|\Delta\omega|$. Otherwise the system forms a lamellar phase. A deeper insight into the phase behavior is gained from analyzing the free energy contributions in the hexagonal and the lamellar phase with the help of the capabilities of the extended SCF theory developed by us.

I. INTRODUCTION

Polymer networks are used in many manufactured materials like rubber[1] or hydrogels[2,3] and are abundant in biological systems.[4–6] One important aspect of this material class is the flexible elastic response on external impacts, which may lead to rather strong reversible changes of the material shape without destruction of the network topology. In many cases, the systems consist of linear polymer chains, which can crosslink either directly via functional groups or with the help of additional crosslinking molecules. More complex structures like the formation of lamellar phases or micelles can be achieved with the help of block copolymer molecules.[7] This article is dedicated to phases of reversibly crosslinked copolymers, studied with the help of self-consistent field (SCF) theory.

Polymer networks have been studied numerically with molecular dynamics[8,9] and Monte Carlo simulations,[10–12] performed on the atomistic scale[8] or with coarse-grained models.[9,11–13] A general problem for these simulations is the typically large ratio between the polymer chain diameter and the average mesh size of the network. On large scales, up to the macroscopic range, polymer networks can be simulated with classical field theories, in which the extension of the polymer material as well as their mechanical and other physical properties are considered by continuous fields and material equations. Recently, we have successfully developed and applied a new phase field model to study the chemically stimulated swelling and shrinking of electrolytic hydrogels.[14] The method is very helpful for studying the interaction of polymer networks with other materials and external impacts on large scales. However, the interactions and configurations of the polymer chains are not directly taken into account; at best, they are incorporated implicitly in the material equations.

The interaction between the polymers and the connectivity of polymer chains can be considered with the SCF theory, which is a well established method for studying polymer chains without crosslinks.[15–19] The method, which was introduced by Edwards[20] and Helfand and Yukiko[21] is based on a partition function that treats the polymers as continuous lines so that rather large polymers can be mimicked. Extended versions of the SCF theory enable the study of strong fluctuations or dynamical systems. Polymer networks with permanent random crosslinks have been studied with the replica field theory.[22–24] A numerical implementation of the replica field method is difficult, since the fields are defined in the replica space. In this article, we study reversibly crosslinked polymer networks with an extended SCF method that we have recently presented.[25,26]

Block copolymers are used for the creation of nanostructured soft matter systems. One application is the creation of polymer shells filled with active agents for a controlled drug delivery and release.[27,28] *AB* diblock copolymers that are built of monomers *A* and *B* with low compatibility may also form long-range nanostructures like lamellar or hexagonal phases,[7] which may be used to design nanomaterials (see Fig. 1). In pure systems of

Address all correspondence to these authors.
[a)]e-mail: thomas.gruhn@uni-bayreuth.de
[b)]e-mail: heike.emmerich@uni-bayreuth.de
This paper has been selected as an Invited Feature Paper.
DOI: 10.1557/jmr.2013.315

https://doi.org/10.1557/jmr.2013.315 Published online by Cambridge University Press

 © Materials Research Society 2013

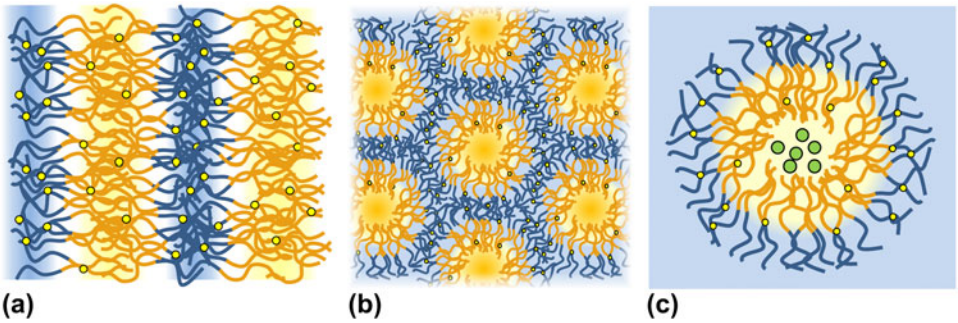


FIG. 1. Structures formed by diblock copolymers with two immiscible types of subchains *A* and *B* (orange and blue). Yellow dots indicate crosslinks. Light yellow and blue background colors indicate solvents compatible with *A* and *B* monomers. Sketches of (a) a lamellar and (b) a hexagonal structure are shown. In (c), the structure of a crosslinked copolymer shell is shown. It serves as a carrier of active agents (green circles) that can be released by breaking the crosslinks.

copolymers, the length scale of the patterns is restricted to the extension of the copolymers. In a mixture of copolymers and two immiscible solvents that have different compatibilities with monomers *A* and *B*, structures on a larger scale may form, in which the copolymers cover the interfaces between the solvents. Introducing two new solvents leads to five new interaction parameters between solvent molecules and monomers of different types. This is avoided in a model system that has been studied numerically in great detail, a system of *AB* diblock copolymers "dissolved" in *A* and *B* homopolymers. The model system has been studied in detail theoretically[16,29,30] and experimentally.[31,32] Many aspects of the model can be transferred to other similar systems, at least qualitatively.

In this work, we investigate nanostructures in $AB + A + B$ polymer systems with reversible crosslinks. The topology of a polymer network and the resulting phase depends crucially on the process of crosslink creation. The formation of networks with permanent crosslinks is a nonequilibrium process if spontaneously formed crosslinks do not break in a reasonable amount of time. However, in some systems, reversible bonds form between the polymers. Noncovalent crosslinks like in Refs. 6 and 33 can form and break on short time scales, so that the network reaches an equilibrium in a canonical ensemble of all possible network configurations and connectivities. If the crosslink strength depends on external parameters like the temperature,[33] the equilibrium structure can be permanentized by a rapid parameter change into the region in which the crosslinks become permanent.

We use an extended SCF theory to study an $AB + A + B$ polymer blend, in which crosslinks can form between the symmetric *AB* copolymers. For *A* and *B* homopolymers, crosslinking between the functional groups is disabled. The polymer blend can be viewed as a model system for reversibly crosslinking amphiphiles dissolved in two demixing solvents. The system depends on various parameters, including the overall crosslink strength z and the crosslink weights ω_A and ω_B of monomers *A* and *B*, respectively. A detailed description of the extended SCF field theory for reversibly crosslinked polymer networks is given in Ref. 25, where the model is tested on an $AB + A + B$ polymer blend with one given set of parameters. A more extensive study of the $AB + A + B$ system with different values of z and $\Delta\omega = \omega_A - \omega_B$ has been recently performed by us.[26] The investigation was restricted to a fraction $\phi_A^{\mathrm{rel}} = 0.6$ of type *A* homopolymers and positive $\Delta\omega$. In the current article, we present a comprehensive phase diagram of the system as a function of the *A* ratio of homopolymers $\phi_A^{\mathrm{rel}} \equiv \phi_A/(\phi_A + \phi_B)$, a relative crosslink strength z_{rel} and the crosslink asymmetry $\Delta\omega$ in the ranges of $0.5 \le \phi_A^{\mathrm{rel}} \le 0.75$, $z_{\mathrm{rel}} \in (0, 2)$, and $\Delta\omega \in (-1, 1)$. By analyzing the contributions to the free energy, we get a deeper insight into the phase behavior of the system, which enhances our previous findings on the model system.

We will start in Sec. II with an introduction into the extended SCF theory for our model system with crosslinked copolymers. Then, in Sec. III, we present the phase diagram as a function of ϕ_A^{rel}, z, and $\Delta\omega$. The diagram is interpreted in Sec. IV by analyzing free energy contributions for the hexagonal and the lamellar phases. Finally, some conclusions are drawn in Sec. V.

II. THEORETICAL BACKGROUND

We consider an incompressible polymer blend with a constant overall density ρ_0 and three types of polymers. Polymers of type *a* and *b* are homopolymers built of *A* and *B* monomers, respectively. Type *c* polymers are diblock copolymers *AB* with half of the chain built of *A* and the other half built of *B* monomers. For simplicity, we assume that all monomers have the same volume. The system includes numbers n_j of polymers $j = a, b, c$. The polymers of type *a*, *b*, and *c* have lengths N_a, N_b, and $N_c \equiv N$, respectively. The stoichiometry of the system is determined by the volume fraction of copolymers,

$$\phi_c = \frac{n_c N}{\sum_{j=a,b,c} n_j N_j} \quad , \tag{1}$$

https://doi.org/10.1557/jmr.2013.315 Published online by Cambridge University Press

and the relative A fraction of homopolymers,

$$\phi_a^{\mathrm{rel}} = \frac{n_a}{n_a + n_b} \quad . \tag{2}$$

The configuration of the kth polymer of type j is given by $\underline{R}_{j,k}(s)$, parameterized by $s \in [0, N_j]$. We assume that all chains in the system have a Gaussian shape distribution $\mathcal{P}(\underline{R}_{j,k}(s))$. The local monomer densities of A and B monomers at position $\underline{x}$ are given by $\hat{\rho}_A(\underline{x})$ and $\hat{\rho}_B(\underline{x})$, respectively. The local density $\hat{\rho}_A(\underline{x}) = \hat{\rho}_A^{(0)}(\underline{x}) + \hat{\rho}_A^{(1)}(\underline{x})$ can be divided into the density $\hat{\rho}_A^{(0)}(\underline{x})$ from type a homopolymers and the density $\hat{\rho}_A^{(1)}(\underline{x})$ from the A part of the copolymers. Analogously, one has $\hat{\rho}_B(\underline{x}) = \hat{\rho}_B^{(0)}(\underline{x}) + \hat{\rho}_B^{(1)}(\underline{x})$. An overview of the notation is given in Fig. 2.

In the absence of crosslinks, the partition function of the system can be written as

$$Z_{nb} = \prod_{j=a,b,c} \frac{1}{n_j!} \prod_{k=1}^{n_j} \int \hat{\mathcal{D}}\{\underline{R}_{j,k}\} \mathcal{P}(\underline{R}_{j,k}(s)) \eta_{nb} \quad , \tag{3}$$

with path integrals $\int \hat{\mathcal{D}}\{\underline{R}_{j,k}\}$ over all configurations of the kth polymer of type j and

$$\eta_{nb} \equiv \delta(\hat{\rho}_A + \hat{\rho}_B - \rho_0) \exp\left(-\frac{1}{\rho_0} \int dx \chi \hat{\rho}_A \hat{\rho}_B\right) \quad . \tag{4}$$

The delta function considers the incompressibility of the system and the exponential term represents the Flory–Huggins interaction with a Flory parameter χ.

Now we consider that reversible crosslinks can form between copolymers. We assume that if a monomer pair $A + A$, $A + B$, or $B + B$ is in contact, a crosslink forms with the probability proportional to $z\omega_A\omega_A$, $z\omega_A\omega_B$, or $z\omega_B\omega_B$, respectively (see Fig. 3). One finds that the partition function can then be written as

$$Z = \prod_{j=a,b,c} \frac{1}{n_j!} \prod_{k=1}^{n_j} \int \hat{\mathcal{D}}\{R_j\} \mathcal{P}(\underline{R}_{j,k}(s)) \eta_{nb} \exp\left(z \int dx \left(\omega_A \hat{\rho}_A^{(1)} + \omega_B \hat{\rho}_B^{(1)}\right)^2\right) \quad . \tag{5}$$

We choose $\omega_A + \omega_B = 1$, so that the crosslink properties are determined by the crosslink strength and the crosslink asymmetry $\Delta\omega \equiv \omega_A - \omega_B$.

In the SCF theory for polymer systems, the Hubbard–Stratonovich (HS) transformation is used to simplify the expression of the partition function in Eq. (5). Below, we present the resulting free energy expression with dimensionless quantities, indicated by a tilde. Dimensionless lengths are defined as $\tilde{x} = x/R_g$ with the gyration radius R_g of a free Gaussian polymer of length N. Dimensionless densities are given by $\tilde{\rho}_A = \rho_A/\rho_0$, while we use dimensionless free energies of the form $\tilde{F} = F \Big/ \left(k_B T \rho_0 R_g^d N^{-1}\right)$. Here kT is the thermal energy and d is the dimension of the system. We use $z_{\mathrm{rel}} = z\rho_0/\chi$ for the crosslink strength. With the HS transformation, one obtains a mean field free energy that can be divided into three terms[25]:

$$\tilde{F}_{\mathrm{tot}} = \tilde{F}_\chi + \tilde{F}_\omega + \tilde{F}_{\mathrm{en}} \quad . \tag{6}$$

The Flory–Huggins part is given by

$$\beta \tilde{F}_\chi = \int \mathrm{d}\tilde{x} \chi N \tilde{\rho}_A \tilde{\rho}_B \quad , \tag{7}$$

with an inverse thermal energy $\beta = (k_B T)^{-1}$. The crosslink contribution can be written as

$$\beta \tilde{F}_\omega = \int \mathrm{d}\tilde{x} z_{\mathrm{rel}} \chi N \left(\omega_A \tilde{\rho}_A^{(1)} + \omega_B \tilde{\rho}_B^{(1)}\right)^2 \quad . \tag{8}$$

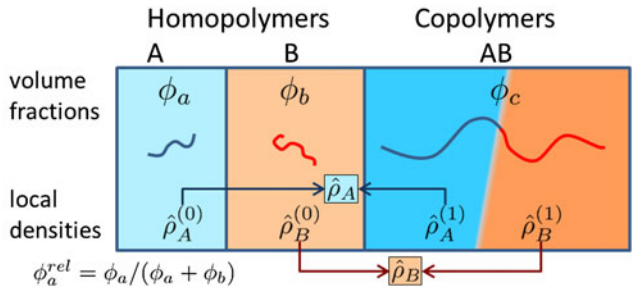


FIG. 2. Summary of important parameters and fields. Homopolymers A and B and copolymers AB have volume fractions ϕ_a, ϕ_b, and ϕ_c, respectively. Local densities of A monomers from homopolymers $\hat{\rho}_A^{(0)}$ and copolymer $\hat{\rho}_A^{(1)}$ sum up to the total local density of A monomers $\hat{\rho}_A = \hat{\rho}_A^{(0)} + \hat{\rho}_A^{(1)}$. The notation of B monomer densities is analogous.

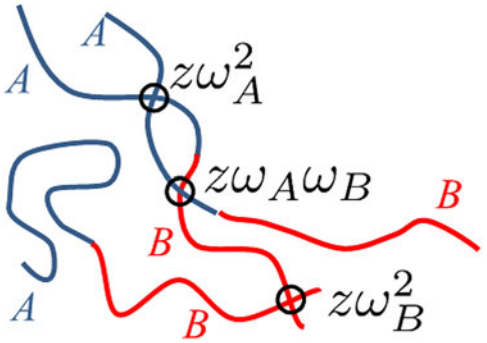


FIG. 3. Reversible crosslinks can form between copolymers. Crosslinks between two monomers of type X and Y with $X, Y \in \{A, B\}$ form with a probability proportional to $z\omega_X\omega_Y$.

https://doi.org/10.1557/jmr.2013.315 Published online by Cambridge University Press

The third term in Eq. (6) considers the entropy of the incompressible polymer blend for given average monomer densities,

$$\beta\tilde{F}_{\mathrm{en}} = -\int \mathrm{d}\tilde{x}\left(\tilde{p}\left(\tilde{\rho}_A + \tilde{\rho}_B - 1\right) + \sum_{m=A}\sum_{j=0,1}\tilde{w}_m^{(j)}\tilde{\rho}_m^{(j)}\right) - \sum_{k=a,b,c}\frac{\phi_k}{N_k}N\ln\frac{Q_k}{n_k} \quad . \tag{9}$$

Here, $\tilde{p}(\underline{x})$ stems from the incompressibility condition and $\tilde{w}_X^{(j)}(\underline{x})$ are auxiliary fields conjugated to the dimensionless equilibrium densities $\tilde{\rho}_X^{(j)}(\underline{x})$ with $X = A, B$ and $j = 0, 1$. Finally, Q_k is the partition function of a single polymer chain of type k fluctuating in the auxiliary fields. A detailed derivation is given in Ref. 25.

In the saddle point approximation, variations of the free energy with respect to $\tilde{w}_X^{(j)}(\underline{x})$, $\tilde{\rho}_X^{(j)}(\underline{x})$, and $\tilde{p}(\underline{x})$ must vanish. The resulting equations can be used to calculate $\tilde{w}_X^{(j)}(\underline{x})$, $\tilde{\rho}_X^{(j)}(\underline{x})$, and $\tilde{p}(\underline{x})$ numerically. An algorithm is described in Ref. 25.

III. PHASE DIAGRAM

The theoretical model, described in the previous section, has been used for a comprehensive study of symmetric $AB + A + B$ polymer blends with reversibly crosslinking copolymers. We consider homopolymers of lengths $N_a = N_b = N/5$, where $N \equiv N_c$ is the length of the copolymers. For the sake of a reasonable computational effort, we restrict the calculations to two-dimensional systems with box lengths L_x and L_y and an area $A = L_xL_y$. We use periodic boundary conditions, a Flory parameter of $\chi N = 11.3$ and a volume fraction $\phi_c = 0.6$ of copolymers. For calculating the single-polymer partition functions, concentration fields, and auxiliary fields, we use a discretization on a square grid in real space. In future calculations, Fourier mode methods may be used to speed up the calculations.

The phase diagram has been studied in the range of $0.5 \le \phi_A^{\mathrm{rel}} \le 0.75$, $0 \le z_{\mathrm{rel}} \le 2$, and $-1 \le \Delta\omega \le 1$. Depending on these parameters, the system formed two different phases in the observed phase region, a hexagonal phase for small z_{rel} and $|\Delta\omega|$ as well as a lamellar phase for suitably large z_{rel} and $|\Delta\omega|$. As shown below, the transition between these two phases is of first order. Close to the phase boundaries, there are strong hysteresis effects and the structure found in the calculations depends on the start configuration. To overcome this problem, we study small systems with a box length ratio of $L_y/L_x = \sqrt{3}$. In this geometry, unit cells of the hexagonal or the lamellar phase can form if L_x is of the correct size. We have varied L_x in the range of $3.0 \le L_x \le 4.8$. The number of grid points was kept fixed. Frequently, we tested that discretization effects are negligible by comparing calculations with different grid sizes up to systems with 960×1663 grid points. From the lowest free energy obtained in the interval $3.0 \le L_x \le 4.8$, we determine the stable phase. Figure 4(a) shows a sequence of free energy plots for $\phi_a^{\mathrm{rel}} = 0.65$, $\Delta\omega = 0.2$, and various values of z. The phase transition occurs at $z_{\mathrm{rel}} \simeq 0.8$. The density of A monomers is shown for a lamellar phase in Fig. 4(b) and for a hexagonal phase in Fig. 4(c).

With the described method, we have calculated the phase diagram as a function of ϕ_a^{rel}, z_{rel}, and $\Delta\omega$. The result is depicted in Fig. 5. It shows phase boundaries between the hexagonal and the lamellar phase for different values of ϕ_a^{rel}. Note that for symmetry reasons, it is sufficient to study $\phi_a^{\mathrm{rel}} \ge 0.5$. For $\phi_a^{\mathrm{rel}} \ge 0.58$, the system shows a hexagonal phase for suitably small z and $|\Delta\omega|$ separated by the phase boundaries from the lamellar phase outside. The phase diagram is not symmetric with respect to $\Delta\omega = 0$ or any other horizontal line $\Delta\omega$ = constant. The asymmetry is caused by the excess of A homopolymers for $\phi_a^{\mathrm{rel}} \ge 0.5$.

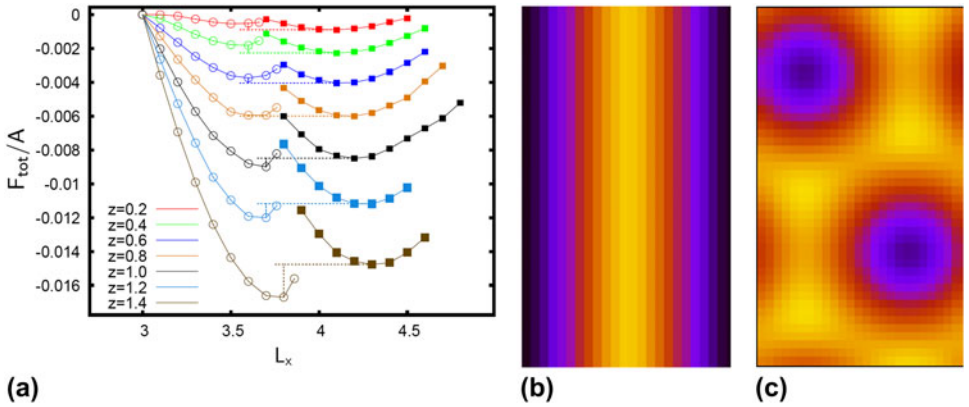


FIG. 4. (a) Free energy of the system as a function of box length L_x with $L_y/L_x = \sqrt{3}$, $\phi_a^{\mathrm{rel}} = 0.65$, $\Delta\omega = 0.2$, and different values of z. Empty circles correspond to the lamellar phase [see unit cell in (b)], filled boxes correspond to the hexagonal phase [see unit cell in (c)]. The dotted lines help to see the differences between the local energy minima of the hexagonal and the lamellar phases.

https://doi.org/10.1557/jmr.2013.315 Published online by Cambridge University Press

The hexagonal phase region expands with increasing ϕ_a^{rel}. For values $\phi_a^{rel} \geq 0.57$, only lamellar phases have been found for $z_{rel} > 0$. For $z_{rel} = 0$, the system always forms a hexagonal phase.

IV. COMPARISON OF FREE ENERGY CONTRIBUTIONS IN THE HEXAGONAL AND THE LAMELLAR PHASE

Analyzing the density distributions of the lamellar and the hexagonal phase, we have found that the system forms more pronounced oscillations of $\rho_A^{(1)}$ and $\rho_B^{(1)}$ in the lamellar phase than in the hexagonal phase. The stronger oscillations in the lamellar phase leads to a more negative crosslink contribution to the free energy, $\tilde{F}_\omega^{lam} < \tilde{F}_\omega^{hex}$. Figure 6 shows the differences $\Delta\tilde{F} = \tilde{F}^{hex} - \tilde{F}^{lam}$ between the hexagonal and the lamellar phase for a system with $\phi_a^{rel} = 0.65$, $\Delta\omega = 0.2$, and various z. For the same systems, free energies $\tilde{F}_{tot}(L_z)$ are shown in Fig. 4(a).

The difference $\Delta\tilde{F}_\omega = \tilde{F}_\omega^{hex} - \tilde{F}_\omega^{lam}$ between the free energy contributions from the crosslinks is positive for all values of z. The sum of the remaining free energy contributions is always lower in the hexagonal phase $\left(\Delta\tilde{F}_{en} + \Delta\tilde{F}_\chi < 0\right)$. In the inset of Fig. 6, $\Delta\tilde{F}_{en}$ and $\Delta\tilde{F}_\chi$ are shown, individually. The absolute value of both quantities is much larger than that of ΔF_{tot}, but $\Delta\tilde{F}_{en}$ and $\Delta\tilde{F}_\chi$ have opposite signs and their sum is of the order of ΔF_{tot}. The value $\Delta\tilde{F}_{en}$ decreases with increasing z_{rel}, whereas $\Delta\tilde{F}_\chi$ gets larger. For $z_{rel} \geq 0.4$, the entropy is larger in the hexagonal state, whereas the Flory–Huggins contribution is more pronounced in the lamellar phase. For a stabile hexagonal phase, the difference between the volume fractions of homopolymers A and B must be suitably large, i.e., ϕ_a^{rel} must be big enough. Then, the entropic free energy contribution $\Delta\tilde{F}_{en}$ profits from the hexagonal structure, in which the circular domains are predominantly filled with B monomers. For larger z_{rel} or $\Delta\omega$, the crosslink contribution dominates. Studying the density distribution in the lamellar phase, one finds that $\tilde{\rho}_A^{(1)}$ and $\tilde{\rho}_B^{(1)}$ oscillates almost symmetrically around $\tilde{\rho}^{(1)}$.

With $\Delta\tilde{\rho}^{(1)} \equiv \tilde{\rho}_A^{(1)} - \tilde{\rho}_B^{(1)}$ the free energy contribution $\tilde{F}_\omega$ can be written as

$$\tilde{F}_\omega = -z\int d\tilde{x}\left(\frac{1+\Delta\omega}{2}\left(\rho^{(1)} + \Delta\rho^{(1)}\right) + \frac{1+\Delta\omega}{2}\left(\rho^{(1)} - \Delta\rho^{(1)}\right)\right)^2 \simeq -\frac{z}{4}\int d\tilde{x}\left(\left(\tilde{\rho}^{(1)}\right)^2 + \Delta\omega^2\left(\Delta\tilde{\rho}^{(1)}\right)^2\right) \quad . \tag{10}$$

For a given lamellar density distribution, $\tilde{F}_\omega$ decreases with increasing z or $|\Delta\omega|$, independent of the sign of $\Delta\omega$. Thus, a demixing of the A and B parts of the copolymers is more favored as z or $|\Delta\omega|$ increases.

It is interesting to compare the phase behavior of our system with that of regular copolymer blends. For the latter systems, the large values of the parameter $N\chi/T$ support a higher degree of order and segregation in the system and counteracts the mixing tendency of the entropy.[29–32] For our system with reversible crosslinks, large values of χ, z, and $|\Delta\omega|$ support a higher degree of order. With this respect, we find that, similar to

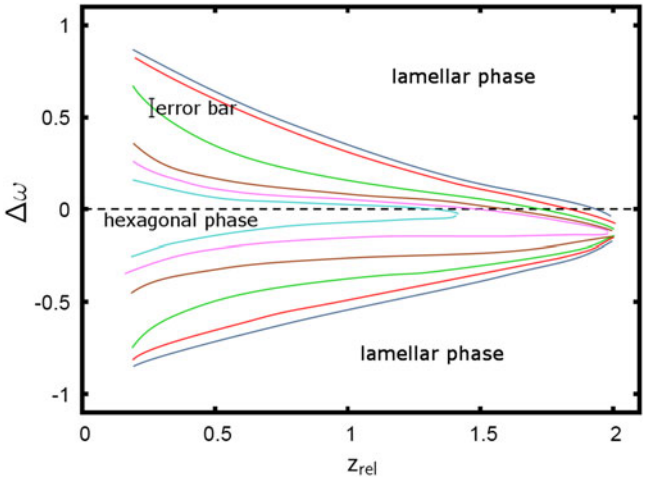


FIG. 5. Phase diagram of the $AB + A + B$ polymer blend: The colored curves denote the phase boundaries between the hexagonal phase on the inside (small $|\Delta\omega|$) and the lamellar phase on the outside. Phase boundaries are shown for $\phi_A = 0.75$ (dark blue), $\phi_A = 0.7$ (red), $\phi_A = 0.65$ (green), $\phi_A = 0.6$ (brown), $\phi_A = 0.59$ (magenta), and $\phi_A = 0.58$ (cyan).

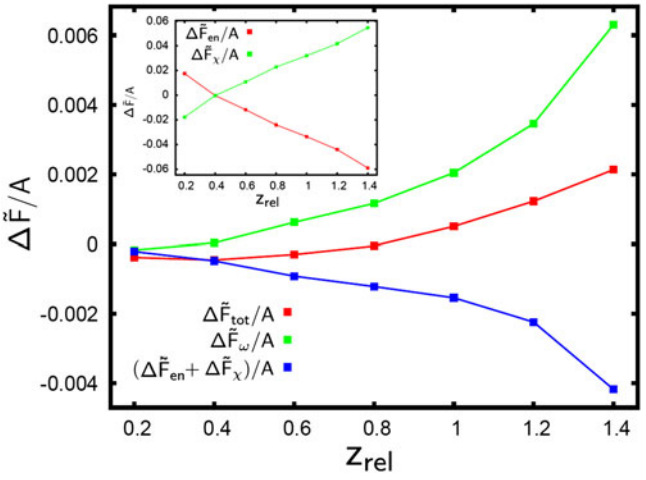


FIG. 6. The total free energy $\tilde{F}_{tot}$ consists of a crosslink part $\tilde{F}_\omega$, a Flory–Huggins part $\tilde{F}_\chi$, and an entropy part $\tilde{F}_{en}$ [see Eq. (6)]. For suitably large crosslink strength z_{rel}, the crosslink free energy F_ω^{hex} in the hexagonal phase is distinctly larger than F_ω^{lam} in the corresponding lamellar phase so that the difference $\Delta\tilde{F}_\omega = \tilde{F}_\omega^{hex} - \tilde{F}_\omega^{lam}$ is distinctly larger than zero. For $z_{rel} > 0.8$, this stabilization of the lamellar phase wins over the remaining free energy contributions $\tilde{F}_{en} + \tilde{F}_\chi$ that favor the hexagonal phase (note that $\Delta\tilde{F}_{en} + \Delta\tilde{F}_\chi = \left(\tilde{F}_{en}^{hex} - \tilde{F}_{en}^{lam}\right) + \left(\tilde{F}_\chi^{hex} + F_\chi^{lam}\right) < 0$). In the inset, $\Delta\tilde{F}_{en}$ and $\Delta\tilde{F}\chi$ are shown, separately. Free energy values are taken from corresponding hexagonal and lamellar phases at the respective local minima of $\tilde{F}_{tot}$, which are shown in Fig. 4(a) for $\phi_a^{rel} = 0.65$, $\Delta\omega = 0.2$, and different values of z. See Sec. IV for a discussion of the free energy contributions.

https://doi.org/10.1557/jmr.2013.315 Published online by Cambridge University Press

regular copolymer blends,[29–32] the lamellar phase is more stable than the hexagonal phase if a high degree of order is favored.

However, phase stability depends sensitively on details of the polymer blend. In our system, an excess of A homopolymers $\left(\phi_A^{\mathrm{rel}} > 0.5\right)$ supports the hexagonal phase, in which the A-rich domains are larger than the circular B-rich domains; the size of the hexagonal part of the phase diagram grows with increasing ϕ_A^{rel}. One might expect the same effect in systems of noncrosslinking block copolymers if the length l_A is larger than the length l_B of the B blocks. Such systems have been studied with the SCF theory.[34] It was found that for a small excess of A monomers, the hexagonal phase is most stable. However, for distinctly longer A blocks $\left(l_A/l_B \gtrsim 0.68\right)$, the lamellar phase is more stable than the hexagonal phase. (In addition, these systems form three-dimensional microphases. For details, we refer to Ref. 34.)

V. CONCLUSIONS

An extended SCF theory has been used to investigate a polymer blend formed by AB diblock copolymers and A and B homopolymers. Reversible crosslinks are considered between the copolymers with a crosslink strength z and a crosslink asymmetry $\Delta\omega = \omega_A - \omega_B$. We obtain a phase diagram as a function of $\phi_a^{\mathrm{rel}} > 0.5$, z_{rel}, and $\Delta\omega$. For $\phi_a^{\mathrm{rel}} < 0.58$ and $z_{\mathrm{rel}} > 0$, only a lamellar phase is found. Otherwise, a hexagonal phase is found for suitably small z_{rel} and $|\Delta\omega|$. With increasing ϕ_a^{rel}, the stoichiometry gets more asymmetric, and the asymmetric hexagonal phase region in the phase diagram grows.

Our studies reveal that the structure of the studied system can be switched from the hexagonal phase to the lamellar phase and back by changing the crosslink properties or the stoichiometry of the system. The first switching method can be achieved with crosslinks that depend on external parameters like the temperature[33] or illumination.[35] The second switching method can be easily achieved by changing the ratio between the volume fractions of A and B homopolymers. Analyzing the free energy contributions for $\phi_a^{\mathrm{rel}} \geq 0.58$, we find that the hexagonal phase has a larger entropic contribution to free energy, whereas the crosslink free energy contribution is stronger in the lamellar phase.

With these studies, we have shown that our extended version of the SCF theory is an excellent tool for a detailed investigation of reversibly crosslinked polymer networks. Many advanced SCF techniques, developed for complex polymer blends without crosslinks, can be combined with our method to study reversibly crosslinked polymer networks with more complex structures.

ACKNOWLEDGMENT

This work was supported by DFG SPP 1259: "Intelligente Hydrogele, modeling and simulation of hydrogel swelling under strong non-equilibrium conditions using the phase-field and phase-field crystal methods" and by DFG SFB 840: "Von Partikulären Nanosystemen zur Mesotechnologie."

REFERENCES

1. V.M. Litvinov, R.O. Orzy, M. Klüppel, M. van Duin, and P.C.M.M. Magusin: Rubber filler interactions and network structure in relation to stress-strain behavior of vulcanized, carbon black filled EPDM. *Macromolecules* **44**, 4887 (2011).
2. D. Buenger, F. Tupoz, and J. Groll: Hydrogels in sensing applications. *Prog. Polym. Sci.* **37**, 1678 (2012).
3. J. Tang, J. Wu, S. Lin, S. Fan, and D. Hu: A multifunctional poly (acrylic acid)/gelatin hydrogel. *J. Mater. Res.* **24**, 1653 (2009).
4. D.A. Fletcher and R.D. Mullins: Cell mechanics and the cytoskeleton. *Nature* **463**, 485 (2010).
5. R.R.R. Vincent, B.W. Mansel, A. Kramer, K. Kroy, and M.A.K. Williams: Micro-rheological behaviour and nonlinear rheology of networks assembled from polysaccharides from the plant cell wall. *New J. Phys.* **15**, 035002 (2013).
6. E. Secchi, T. Roversi, S. Buzzaccaro, L. Piazza, and R. Piazza: Biopolymer gels with "physical" cross-links: Gelation kinetics, aging, heterogeneous dynamics, and macroscopic mechanical properties. *Soft Matter* **9**, 3931 (2013).
7. S-Y. Park, W-H. Sul, and Y-J. Chang: A study on the selectivity of toluene/ethanol mixtures on the micellar and ordered structures of poly(styrene-*b*-4-vinylpyridine) using small-angle x-ray scattering, generalized indirect Fourier transform, and transmission electron microscopy. *Macromolecules* **40**, 3757 (2007).
8. N.B. Shenoga, M. Tsige, S.S. Patnaik, and S.M. Mukhopadhyay: Molecular modeling approach to prediction of thermo-mechanical behavior of thermoset polymer networks. *Macromolecules* **45**, 5307 (2012).
9. Y. Li, M. Kröger, and W.K. Liu: Primitive chain network study on uncrosslinked and crosslinked cis-polyisoprene polymers. *Polymer* **52**, 5867 (2011).
10. M. Quesada-Pérez, J.G. Ibarra-Armenta, and A. Martín-Molina: Computer simulations of thermo-shrinking polyelectrolyte gels. *J. Chem. Phys.* **135**, 094109 (2011).
11. R. Chelakkota and T. Gruhn: Length dependence of crosslinker induced network formation of rods: A Monte Carlo study. *Soft Matter* **8**, 11746 (2012).
12. R. Chelakkot, R. Lipowsky, and T. Gruhn: Self-assembling networks and bundle structures in systems of filaments and crosslinkers: A Monte Carlo study. *Macromolecules* **39**, 7138 (2006).
13. T.H. Weisgraber, R.H. Gee, A. Maiti, D.S. Clague, S. Chinn, and R.S. Maxwell: A mesoscopic network model for permanent set in crosslinked elastomers. *Polymer* **50**, 5613 (2009).
14. D. Li, H.L. Yang, and H. Emmerich: Phase field model simulations of hydrogel dynamics under chemical stimulation. *Colloid Polym. Sci.* **289**, 513 (2011).
15. K. Binder and A. Milchev: Polymer brushes on flat and curved surfaces: How computer simulations can help to test theories and to interpret experiments. *J. Polym. Sci., Part B: Polym. Phys.* **50**, 1515 (2012).
16. J. Wang, M. Müller, and Z-G. Wang: Nucleation in A/B/AB blends: Interplay between microphase assembly and macrophase separation. *J. Chem. Phys.* **130**, 154902 (2009).
17. M. Müller and F. Schmid: Incorporating fluctuations and dynamics in self-consistent field theories for polymer blends. *Adv. Polym. Sci.* **185**, 1 (2005).
18. G.H. Fredrickson, V. Ganesan, and F. Drolet: Field-theoretic computer simulation methods for polymers and complex fluids. *Macromolecules* **35**, 16 (2002).
19. F. Schmid: Self-consistent-field theories for complex fluids. *J. Phys. Condens. Matter* **10**, 8108 (1998).

https://doi.org/10.1557/jmr.2013.315 Published online by Cambridge University Press

20. S.F. Edwards: The statistical mechanics of polymers with excluded volume. *Proc. Phys. Soc.* **85**, 613 (1965).
21. E. Helfand and T. Yukiko: Theory of the interface between immiscible polymers. II. *J. Chem. Phys.* **56**, 3592 (1972).
22. M. Benhamou, A. Derouiche, A. Bettachy, and F. Elhajjaji: Critical microphase properties of crosslinked polymer blends with quenched random impurities. *Eur. Phys. J. E* **34**, 3 (2011).
23. X. Mao, P.M. Goldbart, X. Xing, and A. Zippelius: Soft random solids and their heterogeneous elasticity. *Phys. Rev. E* **80**, 031140 (2009).
24. S. Ulrich, X. Mao, M. Goldbart, and A. Zippelius: Elasticity of highly cross-linked random networks. *Europhys. Lett.* **76**, 677 (2006).
25. D. Li, T. Gruhn, and H. Emmerich: Mean field theory for a reversibly crosslinked polymer network, *J. Chem. Phys.* **137**, 024906 (2012).
26. T. Gruhn, D. Li, and H. Emmerich: Calculating structural properties of reversibly crosslinked polymer systems using self-consistent field theory. *Prog. Colloid Polym. Sci.*, submitted.
27. C. Wu, A. Ying, and S. Ren: Fabrication of polymeric micelles with core–shell–coronastructure for applications in controlled drug release. *Colloid. Polym. Sci.* **291**, 827 (2013).
28. J. Yue, R. Wang, S. Liu, S. Wu, Z. Xie, Y. Huang, and X. Jing: Reduction-responsive shell-crosslinked micelles prepared from Y-shaped amphiphilic block copolymers as a drug carrier. *Soft Matter* **8**, 7426 (2012).
29. E. Helfand: Theory of inhomogeneous polymers: Fundamentals of the Gaussian random-walk model, *J. Chem. Phys.* **62**, 999 (1975).
30. D. Düchs, V. Ganesan, G.H. Fredrickson, and F. Schmid: Fluctuation effects in ternary AB+A+B polymeric emulsions, *Macromolecules* **36**, 9237 (2003).
31. F.S. Bates, W.W. Maurer, P.M. Lipic, M.A. Hillmyer, K. Almdal, K. Mortensen, G.H. Fredrickson, and T.P. Lodge: Polymeric bicontinuous microemulsions, *Phys. Rev. Lett.* **79**, 849 (1997).
32. M.A. Hillmyer, W.W. Maurer, T.P. Lodge, F.S. Bates, and K.J. Almdal: Model bicontinuous microemulsions in ternary homopolymer/block copolymer blends, *Phys. Chem.* **103**, 4814 (1999).
33. J. Adelsberger, E. Metwalli, A. Diethert, I. Grillo, A.M. Bivigou-Koumba, A. Laschewsky, P. Müller-Buschbaum, and C. M. Papadakis: Kinetics of collapse transition and cluster formation in a thermoresponsive micellar solution of P(S-*b*-NIPAM-*b*-S) induced by a temperature jump. *Macromol. Rapid Commun.* **33**, 254 (2012).
34. M.W. Matsen and F.S. Bates: Unifying weak- and strong-segregation block copolymer theories, *Macromolecules* **29**, 1091 (1996).
35. W.T.S. Huck: Materials chemistry: Polymer networks take a bow. *Nature* **472**, 425 (2011).

https://doi.org/10.1557/jmr.2013.315 Published online by Cambridge University Press